Modern Physics Letters B Vol. 37, No. 29 (2023) 2350119 (13 pages) © World Scientific Publishing Company DOI: 10.1142/S0217984923501191



Non-Fermi liquid behavior in a simple model of Fermi arcs and pseudogap

Ruojun Wang*

Department of Physics and National High Magnetic Field Laboratory, Florida State University Tallahassee, FL 32306, USA rw19f@fsu.edu

Kun Yang

Magnetic Field Laboratory, Florida State University, Tallahassee, FL 32306, USA kunyang@magnet.fsu.edu

Received 25 January 2023 Revised 31 March 2023 Accepted 16 April 2023 Published 28 June 2023

In this paper, we consider a perturbed version of a very simple and exactly solvable model that supports Fermi arcs and pseudogap in its ground state and excitation spectrum, which includes Hubbard-like interactions in both momentum and real spaces. We find that the combined effects give rise to non-Fermi liquid behavior in the electron self-energy. This points to a novel mechanism that leads to non-Fermi liquid behavior, which is of strong current interest in the context of strongly correlated metals, that often become superconductors. Comparison will be made with phenomenology of high-temperature cuprate superconductors.

Keywords: Strongly correlated electrons; non-Fermi liquid; Feynman diagrammatic analysis.

1. Introduction

The normal state of high transition temperature (T_c) cuprate superconductors is known to exhibit non-Fermi liquid behavior in the underdoped regime. Among their mysterious properties, they support pseudogaps and Fermi arcs instead of closed Fermi surfaces of ordinary Fermi liquid. Non-Fermi liquid behavior is also manifested in the lack of coherence in quasiparticle excitations and unusual transport properties. Understanding such non-Fermi liquid physics is an exciting challenge we face.

^{*}Corresponding author.

In an earlier paper,⁴ one of us introduced an extremely simple and exactly solvable model, and showed that Fermi arcs and pseudogap appear very naturally (and hand-in-hand) in its ground state and excitation spectrum. That model is a variant of a model introduced by Hatsugai and Kohmoto (HK)⁵ (a model similar to that of HK was considered earlier by Baskaran⁶).

An unusual property of this model⁴ (which we refer to as HKY model from now on) is that all quasiparticle and quasihole excitations are sharp, albeit being gapped in the pseudogap region. This is, of course, opposite to non-Fermi liquids where quasiparticle and quasihole excitations are incoherent, rendering the electron spectral functions very broad. The sharpness of the electron spectral function in the HKY model is the consequence of the fact that its interaction is local in momentum space and only gives rise to forward scattering. To remove this artifact, in this paper, we perturb the HKY model with a (real space) Hubbard interaction, and calculate its contribution to electron self-energy. We demonstrate that the combined effects of the Hubbard and HKY interactions render the quasiparticle and quasihole excitations incoherent, consistent with the cuprate phenomenology. More importantly, our results point to a novel mechanism that leads to non-Fermi liquid behavior, which is of strong current interest in the context of strongly correlated metals, where related non-Fermi liquid behaviors are often observed.

The rest of the paper is organized as follows. In Sec. 2, we introduce the HKY model perturbed by the Hubbard interaction, and its mean-field solution which gives rise to Fermi arcs and pseudogap regions. In Sec. 3, we set up the Feynman rules for perturbative treatments of interactions, and demonstrate that all non-vanishing diagrams involving HKY interactions form particle—particle and particle—hole ladders that can be summed exactly. In Sec. 4, we calculate the electron self-energy to the second order in Hubbard interaction, and demonstrate its imaginary part remains finite in the low-energy limit, resulting in non-Fermi liquid behavior. A brief summary is provided in Sec. 5.

2. Model and Mean-Field Solution

We start by considering the HKY model:

$$H_{\rm HKY} = \sum_{\mathbf{k}} [\epsilon_{\mathbf{k}} (\hat{n}_{\mathbf{k}\uparrow} + \hat{n}_{\mathbf{k}\downarrow}) + u_{\mathbf{k}} \hat{n}_{\mathbf{k}\uparrow} \hat{n}_{\mathbf{k}\downarrow}], \tag{1}$$

where $\epsilon_{\mathbf{k}}$ is the single-particle energy, $n_{\mathbf{k}\sigma} = c_{\mathbf{k}\sigma}^{\dagger} c_{\mathbf{k}\sigma}$ is the fermion occupation for momentum \mathbf{k} and spin $\sigma = \uparrow, \downarrow$, and $u_{\mathbf{k}}$ is the interaction energy between the spin-up and spin-down particles. When $u_{\mathbf{k}}$ is a constant, the model is reduced to the HK model.⁵

While (1) is exactly solvable, in preparation for the breakdown of solvability once the (real space) Hubbard (or any other generic) interaction is introduced we first introduce a mean-field solution to (1), which we will use as the starting point for perturbation theory later on. Note that this mean-field solution is exact for the ground state and single-particle/hole excitations. We separate the operator $\hat{n}_{\mathbf{k}\sigma}$ into its expectation value and fluctuation:

$$\hat{n}_{\mathbf{k}\sigma} = n_{\mathbf{k}\sigma} + \delta \hat{n}_{\mathbf{k}\sigma},\tag{2}$$

where $n_{\mathbf{k}\sigma} = \langle \hat{n}_{\mathbf{k}\sigma} \rangle$, and write the Hamiltonian as

$$H_{HKV} = H_0 + H_1 + H_2, \tag{3}$$

such that

$$H_0 = \sum_{\mathbf{k}\sigma} E_{\mathbf{k}\sigma} \hat{n}_{\mathbf{k}\sigma},\tag{4}$$

$$H_1 = -\sum_{\mathbf{k}\sigma} n_{\mathbf{k},-\sigma} u_{\mathbf{k}} \hat{n}_{\mathbf{k}\sigma},\tag{5}$$

$$H_2 = \sum_{\mathbf{k}} u_{\mathbf{k}} \hat{n}_{\mathbf{k}\uparrow} \hat{n}_{\mathbf{k}\downarrow},\tag{6}$$

where $E_{\mathbf{k}\sigma} = \epsilon_{\mathbf{k}} + n_{\mathbf{k},-\sigma}u_{\mathbf{k}}$, is the single-particle energy within the Hartree approximation and we denote $-\sigma$ as the opposite spin of σ . The ground state of H_0 , which is also the *exact* ground state of H_{HKY} , has the following occupation pattern:

$$n_{\mathbf{k}} = \begin{cases} 0, & \epsilon_{\mathbf{k}} > 0 & \text{and} & \epsilon_{\mathbf{k}} + u_{\mathbf{k}} > 0, \\ 1, & \epsilon_{\mathbf{k}} < 0 & \text{and} & \epsilon_{\mathbf{k}} + u_{\mathbf{k}} > 0, \\ 2, & \epsilon_{\mathbf{k}} < 0 & \text{and} & \epsilon_{\mathbf{k}} + u_{\mathbf{k}} < 0 \end{cases}$$
 (7)

and those regions are distinguished by the surfaces defined by

$$\epsilon_{\mathbf{k}} = 0,$$
 (8)

$$\epsilon_{\mathbf{k}} + u_{\mathbf{k}} = 0, \tag{9}$$

$$u_{\mathbf{k}} = 0. \tag{10}$$

As pointed out in Ref. 4, we have pseudo-Fermi surfaces across which occupation numbers change by 2 ($\Delta n_{\rm k}=2$) where there is a single-particle energy gap of $|u_{\rm k}|/2$ (i.e. pseudogap), and Fermi-arcs across which occupation numbers change by 1 ($\Delta n_{\rm k}=1$) with no such gap. In the region with $n_{\rm k}=1$, each state can be occupied by either spin-up or spin-down fermions, resulting in a massive degeneracy. In order to remove this degeneracy, we can introduce an infinitesimal Zeeman splitting Δ_Z between the spin-up and spin-down fermions:

$$H_Z = \Delta_Z \sum_{\mathbf{k}} n_{\mathbf{k}\uparrow} \tag{11}$$

$$= \frac{\Delta_Z}{2} \sum_{\mathbf{k}} (n_{\mathbf{k}\uparrow} - n_{\mathbf{k}\downarrow}) + \frac{\Delta_Z}{2} \sum_{\mathbf{k}} (n_{\mathbf{k}\uparrow} + n_{\mathbf{k}\downarrow}), \tag{12}$$

so that the $n_{\bf k}=1$ regions are occupied by the spin-down fermions only in the ground state.⁴ The occupation conditions in $n_{\bf k}=0$ and $n_{\bf k}=2$ region would not be affected

by the Zeeman splitting and remain as they are in Eq. (7). The Fermi arcs are then the Fermi surfaces for spin-up and spin-down fermions, respectively, albeit they are not closed (hence arcs). The single-particle Green's function of H_0 , again the same as the exact Green's function of $H_{\rm HKY}$ is

$$G_{\sigma}^{0}(\omega \mathbf{k}) = \frac{(1 - n_{\mathbf{k}\sigma})(1 - n_{\mathbf{k},\sigma})}{\omega + i\eta - \hbar^{-1}\epsilon_{\mathbf{k}}} + \frac{(1 - n_{\mathbf{k}\sigma})n_{\mathbf{k},-\sigma}}{\omega + i\eta - \hbar^{-1}(\epsilon_{\mathbf{k}} + u_{\mathbf{k}})} + \frac{n_{\mathbf{k},-\sigma}(1 - n_{\mathbf{k},\sigma})}{\omega - i\eta - \hbar^{-1}\epsilon_{\mathbf{k}}} + \frac{n_{\mathbf{k},-\sigma}n_{\mathbf{k},-\sigma}}{\omega - i\eta - \hbar^{-1}(\epsilon_{\mathbf{k}} + u_{\mathbf{k}})}$$

$$(13)$$

$$= \frac{(1 - n_{\mathbf{k}\sigma})}{\omega + i\eta - \hbar^{-1}E_{\mathbf{k}\sigma}} + \frac{n_{\mathbf{k}\sigma}}{\omega - i\eta - \hbar^{-1}E_{\mathbf{k},-\sigma}},\tag{14}$$

where ω is the frequency of the particle, \mathbf{k} is the momentum of it, and η is an infinitesimal positive. We have already defined $n_{\mathbf{k}\sigma}$, $E_{\mathbf{k}\sigma}$, $\epsilon_{\mathbf{k}}$, $u_{\mathbf{k}}$ earlier where Eqs. (1) and (4)–(6) appear. Here, $n_{\mathbf{k},-\sigma}$ gives an opposite spin compared to $n_{\mathbf{k}\sigma}$ so that we have $(1-n_{\mathbf{k}\sigma})(1-n_{\mathbf{k},-\sigma})$ stands for the $n_{\mathbf{k}\sigma}=0$ region, $n_{\mathbf{k}\sigma}n_{\mathbf{k},-\sigma}$ stands for the $n_{\mathbf{k}\sigma}=2$ region, and $(1-n_{\mathbf{k}\sigma})n_{\mathbf{k},-\sigma}$, together with $n_{\mathbf{k}\sigma}(1-n_{\mathbf{k},-\sigma})$, stands for the $n_{\mathbf{k}\sigma}=1$ region.

In addition to the Hamiltonian in Eq. (3), we consider a perturbing Hubbard interaction:

$$H_{\text{Hubbard}} = V \sum_{i} \hat{n}_{i\uparrow} \hat{n}_{i\downarrow} = \frac{V}{N} \sum_{\mathbf{k}\mathbf{k'}\mathbf{q}} c_{\mathbf{k}+\mathbf{q}\uparrow}^{\dagger} c_{\mathbf{k'}-\mathbf{q}\downarrow}^{\dagger} c_{\mathbf{k}\uparrow}, \tag{15}$$

where V is the interaction strength, i is site index, N is system size, \mathbf{k} , \mathbf{k}' and \mathbf{q} are the variables for momenta, and $c_{\mathbf{k}}^{\dagger}$ and $c_{\mathbf{k}}$ are the creation and annihilation operators as we defined earlier in $n_{\mathbf{k}\sigma} = c_{\mathbf{k}\sigma}^{\dagger} c_{\mathbf{k}\sigma}$ for Eq. (1). Hence, the full Hamiltonian we would like to consider is the sum of the HKY Hamiltonian and the Hubbard interaction:

$$H = H_{\text{HKY}} + H_{\text{Hubbard}} = H_0 + H', \tag{16}$$

where we treat H_1 , H_2 , and H_{Hubbard} perturbatively such that

$$H' = H_1 + H_2 + H_{\text{Hubbard}}.$$
 (17)

3. Feynman Rules and Ladder Sums

The Feynman rules can be established following standard textbooks. We start by considering the perturbative expansion of the exact single-particle Green's function given by the full Hamiltonian in Eq. (16):

$$iG_{\sigma}(\mathbf{k}, t - t') = \frac{1}{D} \sum_{\nu=0}^{\infty} \left(-\frac{i}{\hbar} \right)^{\nu} \frac{1}{\nu!} \int_{-\infty}^{\infty} dt_{1} \dots \int_{-\infty}^{\infty} dt_{\nu} \times \langle \Phi_{0} | T[H'(t_{1}) \dots H'(t_{\nu}) c_{\mathbf{k}\sigma}(t) c_{\mathbf{k}\sigma}^{\dagger}(t')] | \Phi_{0} \rangle, \tag{18}$$

where ν is an integer, $|\Phi_0\rangle$ is the ground state of H_0 , and the denominator D results in all disconnected diagrams containing the components that are not connected to the

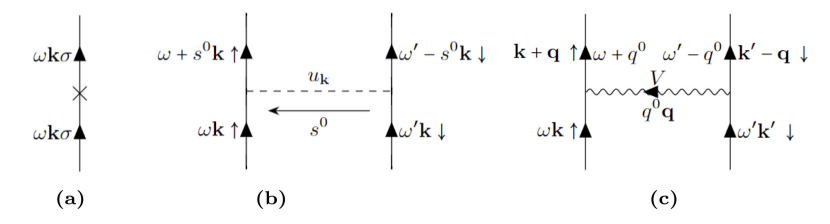


Fig. 1. Vertices given by the interaction resulting from (a) H_1 , (b) H_2 , and (c) H_{Hubbard} .

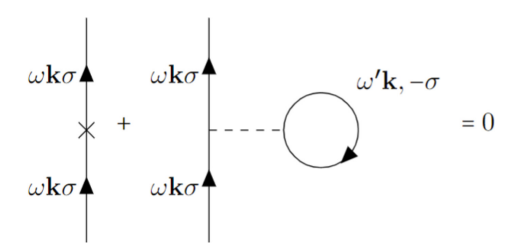


Fig. 2. An example of diagrams that are not part of the particle–particle or particle–hole ladder of HKY interaction (H_2) . All such diagrams vanish.

rest of the diagram by any lines. We apply Wick's theorem based on this expansion so that all the disconnected diagrams could be ignored. In addition, we introduce a solid line to denote the unperturbed Green's function $G_{\sigma}^{0}(\omega, \mathbf{k})$ in Eq. (13), a cross symbol to denote the interaction given by H_{1} in Eq. (5), a dashed line to denote the one given by H_{2} in Eq. (6), and a wavy line to denote the Hubbard interaction in Eq. (15). Hence, it is necessary to consider those three kinds of vertices in Fig. 1. In terms of these diagrammatic components, we find the diagrams in Fig. 2 cancel each other, where the second one is the Hartree diagram in terms of the H_{2} interaction. Note this cancellation occurs not only when they stand alone in the first-order diagram illustrated here, but also when they are embedded in higher-order diagrams. This cancellation, guaranteed by the self-consistent Hartree condition, is a significant simplification, as we can now drop all diagrams that involve the cross symbol given by Fig. 1(a) and/or a Hartree bubble. Other than this simplification, the Feynman rules are the same as the usual ones.⁷

In addition to Fig. 2, another major simplification is all other contributions from H_2 interaction can be organized as particle—particle and particle—hole ladder diagrams illustrated in Figs. 3 and 4. The first line of the equation in Fig. 4 includes all particle—particle crossing diagrams, which are equivalent to the particle—hole ladder diagrams on the following line. Figures 3 and 4 are the only nonzero contributions given by the H_2 term. This is because H_2 only gives rise to forward scattering, and cannot create particle—hole pairs. Also for this reason, these ladder diagrams can be summed up easily because they form geometric series. To see this, we inspect the

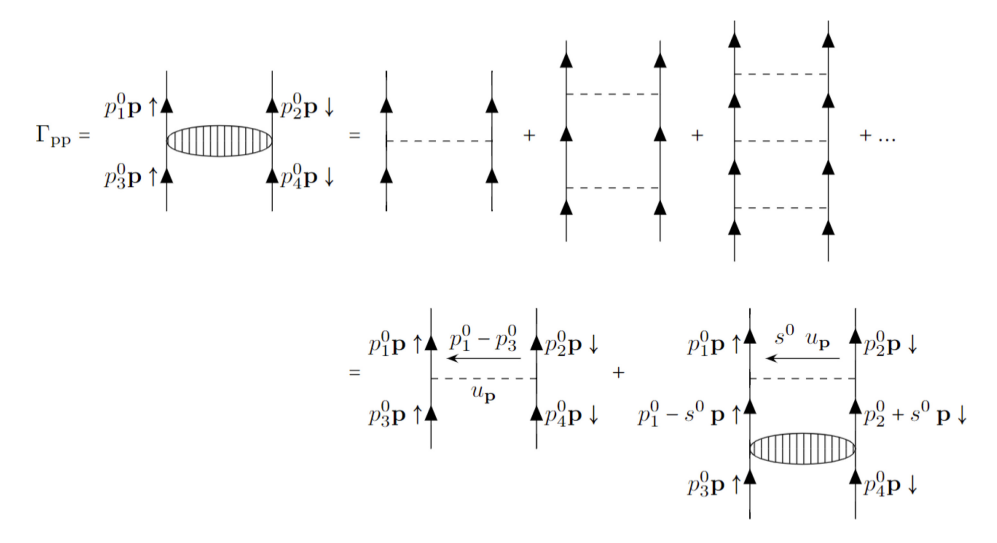


Fig. 3. Particle-particle ladder diagrams.

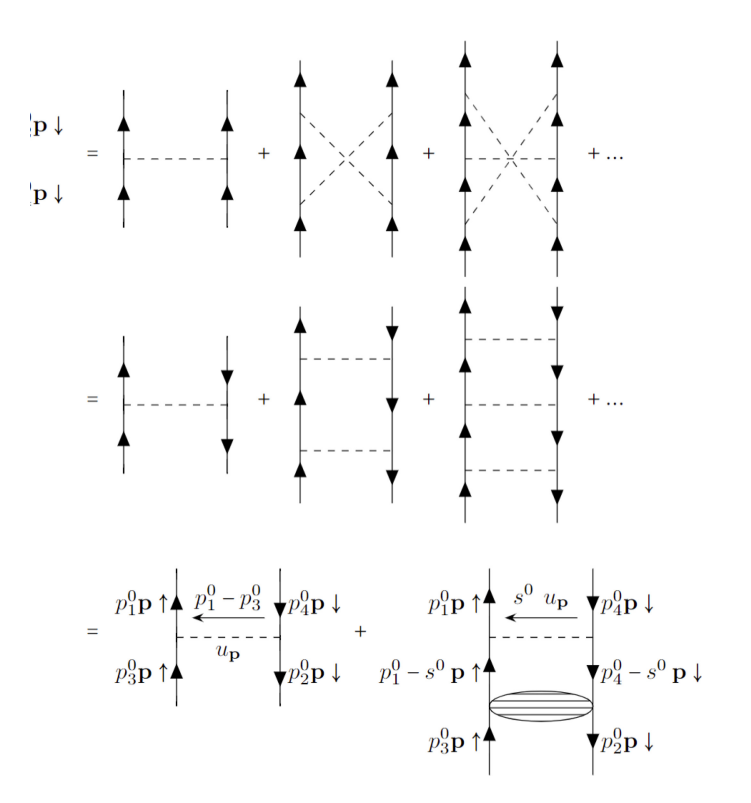


Fig. 4. Particle-hole ladder diagrams.

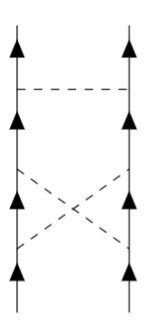


Fig. 5. An example of diagrams that are not part of the particle–particle or particle–hole ladder of HKY interaction (H_2) . All such diagrams vanish.

corresponding Bethe–Salpeter equations⁷

$$\Gamma_{\text{pp}}(p_{1}^{0} + p_{2}^{0}, \mathbf{p})
= u(\mathbf{p}) + u(\mathbf{p})\Gamma(p_{1}^{0} + p_{2}^{0}, \mathbf{p}) \int \frac{dq^{0}}{2\pi} G_{\sigma}^{0} \left(\frac{p_{1}^{0} + p_{2}^{0}}{2} + q^{0}, \mathbf{p}\right) G_{-\sigma}^{0}
\times \left(\frac{p_{1}^{0} + p_{2}^{0}}{2} - q^{0}, \mathbf{p}\right),$$
(19)

and

$$\Gamma_{\rm ph}(p_1^0 - p_4^0, \mathbf{p})
= u(\mathbf{p}) + u(\mathbf{p})\Gamma(p_1^0 - p_4^0, \mathbf{p}) \int \frac{dq^0}{2\pi} G_{\sigma}^0 \left(\frac{p_1^0 - p_4^0}{2} + q^0, \mathbf{p}\right) G_{-\sigma}^0
\times \left(q^0 - \frac{p_1^0 - p_4^0}{2}, \mathbf{p}\right),$$
(20)

where p_1^0 , p_2^0 and p_4^0 are the frequencies carried by the external propagators. Due to the forward-scattering nature, there is no momentum integral, as a result, Γ does not enter the integrals on the right-hand side, allowing the integrals to be carried out explicitly, yielding

$$\Gamma_{\rm pp}(p_1^0 - p_2^0, \mathbf{p}) = \frac{u(\mathbf{p})(1 - n_{\mathbf{p}\sigma})(1 - n_{\mathbf{p}, -\sigma})}{1 - \frac{u(\mathbf{p})}{\hbar(p_1^0 + p_2^0) - (E_{\mathbf{p}\sigma} + E_{\mathbf{p}, -\sigma}) + i\eta}} + \frac{u(\mathbf{p})n_{\mathbf{p}\sigma}n_{\mathbf{p}, -\sigma}}{1 + \frac{u(\mathbf{p})}{\hbar(p_1^0 + p_2^0) - (E_{\mathbf{p}\sigma} + E_{\mathbf{p}, -\sigma}) - i\eta}}, \quad (21)$$

$$\Gamma_{\rm ph}(p_1^0 - p_4^0, \mathbf{p}) = \frac{u(\mathbf{p})(1 - n_{\mathbf{p}\sigma})n_{\mathbf{p}, -\sigma}}{1 - \frac{u(\mathbf{p})}{\hbar(p_1^0 - p_4^0) - (E_{\mathbf{p}\sigma} - E_{\mathbf{p}, -\sigma}) + i\eta}} + \frac{u(\mathbf{p})n_{\mathbf{p}\sigma}(1 - n_{\mathbf{p}, -\sigma})}{1 + \frac{u(\mathbf{p})}{\hbar(p_1^0 - p_4^0) - (E_{\mathbf{p}\sigma} - E_{\mathbf{p}, -\sigma}) - i\eta}}.$$
 (22)

All other diagrams (which inevitably mix particle–particle and particle–hole ladders) vanish, an example of which is shown in Fig. 5. This is due to the restrictions on the occupations in Eqs. (21) and (22), where we only have the combinations of $n_{\mathbf{p}\sigma}n_{\mathbf{p},-\sigma}$, $(1-n_{\mathbf{p}\sigma})(1-n_{\mathbf{p},-\sigma})$ for the former, and $(1-n_{\mathbf{p}\sigma})n_{\mathbf{p},-\sigma}$, $n_{\mathbf{p}\sigma}(1-n_{\mathbf{p},-\sigma})$ for the latter.

4. The Self-Energy Diagrams

In this section, we study the electron self-energy $\Sigma_{\sigma}(\omega, \mathbf{k})$, especially its imaginary part, which tells us the decay rate and the broadening of the electron spectral function measured in the angle-resolved photoemission spectroscopy (ARPES):

$$\frac{1}{\tau} = \text{Im}\Sigma_{\sigma}(\omega, \mathbf{k}). \tag{23}$$

We evaluate the self-energy diagrams to the second order of Hubbard interaction (V^2) , which is the lowest order that gives rise to an imaginary part. We will, however, include all contributions from HKY interaction, using the ladder sums performed in the previous section.

The simplest diagram is the one with Hubbard interaction only (Fig. 6(a)). Its imaginary part is

$$\operatorname{Im}\Sigma_{\sigma}^{6(a)}(\omega, \mathbf{k}) = V^{2} \int \frac{d^{2}k'}{(2\pi)^{2}} \frac{d^{2}q}{(2\pi)^{2}} \delta(\omega + E_{\mathbf{k}', -\sigma} + E_{\mathbf{k}' - \mathbf{q}, -\sigma} - E_{\mathbf{k} + \mathbf{q}, \sigma})$$

$$\times \left[(1 - n_{\mathbf{k}\sigma}) n_{\mathbf{k} + \mathbf{q}, \sigma} (1 - n_{\mathbf{k}', -\sigma}) n_{\mathbf{k}' - \mathbf{q}, -\sigma} - n_{\mathbf{k}\sigma} (1 - n_{\mathbf{k} + \mathbf{q}, \sigma}) n_{\mathbf{k}', -\sigma} (1 - n_{\mathbf{k}' - \mathbf{q}, -\sigma}) \right], \tag{24}$$

which yields the familiar Fermi liquid result near the (pseudo) Fermi surface:

$$Im \Sigma_{\sigma}^{6(a)}(\omega, \mathbf{k}) \approx -D^3 V^2(\hbar \omega)^2, \tag{25}$$

where D is the density of states at the non-interacting Fermi level. We note however this results in much more broadening in the pseudogap region as the quasiparticle energy $\hbar\omega \sim |u|$ is bounded below by the size of the pseudogap, compared to that near the Fermi arcs where $\hbar\omega$ can be arbitrary small. This is consistent with the cuprate phenomenology.

We now turn to the diagrams that involve HKY interaction (H_2) . Those diagrams are in Fig. 6. Here, we present the calculation on the self-energy diagram given by Fig. 6(b) as an example. A full calculation on each diagram is presented in the appendix of the arXiv version.¹²

After performing the frequency integrals, the corresponding imaginary part of Fig. 6(b) takes the following form:

$$\operatorname{Im}\Sigma_{\sigma}^{6(b)}(\omega, \mathbf{k}) = i^{6}\pi V^{2} \int \frac{d^{2}q}{(2\pi)^{2}} \{ [\delta(\omega + E_{-\mathbf{k}+2\mathbf{q},-\sigma} - E_{\mathbf{q}\sigma} - E_{\mathbf{q},-\sigma}) \\
- \delta(\omega + E_{-\mathbf{k}+2\mathbf{q},-\sigma} - E_{\mathbf{q}\sigma} - E_{\mathbf{q},-\sigma} - u_{\mathbf{q}}] (1 - n_{\mathbf{q}\sigma}) \\
\times (1 - n_{\mathbf{q},-\sigma}) n_{-\mathbf{k}+2\mathbf{q},-\sigma} - [\delta(\omega + E_{-\mathbf{k}+2\mathbf{q},-\sigma} - E_{\mathbf{q}\sigma} - E_{\mathbf{q},-\sigma}) \\
- \delta(\omega + E_{-\mathbf{k}+2\mathbf{q},-\sigma} - E_{\mathbf{q}\sigma} - E_{\mathbf{q},-\sigma} + u_{\mathbf{q}})] n_{\mathbf{q}\sigma} n_{\mathbf{q},-\sigma} (1 - n_{-\mathbf{k}+2\mathbf{q},-\sigma}) \}.$$
(26)

Note that compared to Eq. (24) we have one *fewer* momentum integral to perform, despite the extra loop. This is due to the fact HKY interaction forces the propagators coupled by it to have the same momentum. This simplification changes the phase space constraints significantly and enhances Im Σ , as we demonstrate in the following.

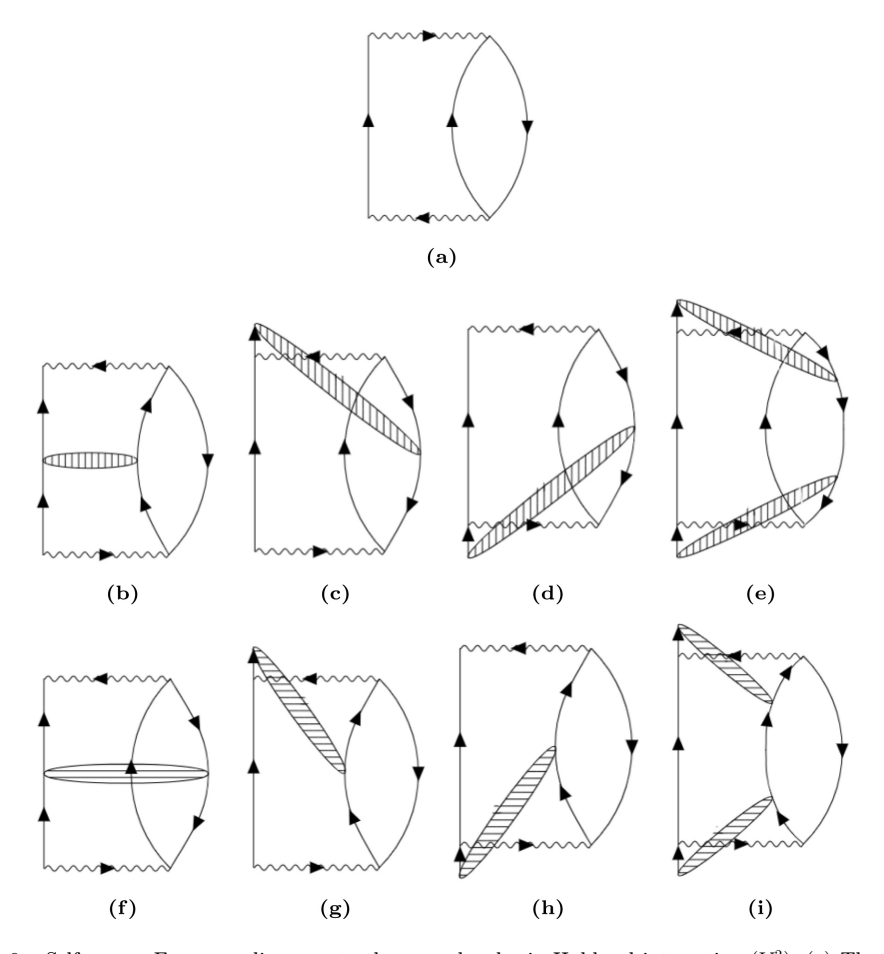


Fig. 6. Self-energy Feynman diagrams to the second order in Hubbard interaction (V^2) . (a) The self-energy diagrams in the second order with Hubbard interaction only. (b)–(i) The self-energy diagrams with both Hubbard and the HKY (H_2) interactions.

To bring Eq. (26) to a form closer to Eq. (24), letting $-\mathbf{k} + 2\mathbf{q} \to \mathbf{q}'$, we treat \mathbf{q}' as an additional integration variable, compensated by an additional delta function. Rewrite the integrals in terms of the polar coordinates such that $(q_x, q_y) = (q\cos\phi, q\sin\phi)$ and $(q'_x, q'_y) = (q'\cos\phi', q'\sin\phi')$. Equation (26) becomes

$$\operatorname{Im}\Sigma_{\sigma}^{6(b)}(\omega, \mathbf{k}) = i^{6}\pi V^{2} \frac{1}{(2\pi)^{2}} \int q dq q' dq' d\phi d\phi' \frac{1}{q'} \delta(q' - |-\mathbf{k} + 2\mathbf{q}|) \delta(\phi' - \phi_{-\mathbf{k} + 2\mathbf{q}})$$

$$\times \{ [\delta(\omega + E_{\mathbf{q}', -\sigma} - 2\epsilon_{\mathbf{q}}) - \delta(\omega + E_{\mathbf{q}', -\sigma} - 2\epsilon_{\mathbf{q}} - u_{\mathbf{q}})] \theta(\epsilon_{\mathbf{q}})$$

$$\times \theta(-E_{\mathbf{q}', -\sigma}) - [\delta(\omega + E_{\mathbf{q}', -\sigma} - 2\epsilon_{\mathbf{q}} - 2u_{\mathbf{q}})$$

$$- \delta(\omega + E_{\mathbf{q}', -\sigma} - 2\epsilon_{\mathbf{q}} - 2u_{\mathbf{q}} + u_{\mathbf{q}})]$$

$$\times \theta(-\epsilon_{\mathbf{q}} - u_{\mathbf{q}}) \theta(E_{\mathbf{q}', -\sigma}) \}. \tag{27}$$

We transform the integral from $\int q dq q' dq'$ to $\int d\epsilon dE' J(\epsilon, E', \phi, \phi')$ and $\int dE dE' d\phi d\phi'$, where $\epsilon = \epsilon_{\mathbf{q}}$, $E = \epsilon_{\mathbf{q}} + u_{\mathbf{q}}$, and $E' = E_{\mathbf{q}', -\sigma}$, and the Jacobian

$$J(\epsilon, E', \phi, \phi') = q \frac{\partial q}{\partial \epsilon} q' \frac{\partial q'}{\partial E'} = D(\epsilon, \phi) D(E', \phi'), \tag{28}$$

$$J(E, E', \phi, \phi') = q \frac{\partial q}{\partial E} q' \frac{\partial q'}{\partial E'} = D(E, \phi) D(E', \phi'), \tag{29}$$

with the angle-dependent density of states

$$D(\epsilon, \phi) = q \frac{\partial q}{\partial \epsilon},\tag{30}$$

$$D(E,\phi) = q \frac{\partial q}{\partial E},\tag{31}$$

$$D(E', \phi') = q' \frac{\partial q'}{\partial E'}.$$
 (32)

In a two-dimensional system, it is a good approximation to treat them as a constant in terms of density of states D:

$$D(\epsilon, \phi)D(E', \phi') \approx D(E, \phi)D(E', \phi') \approx (2\pi D)^2.$$
 (33)

Equation (27) then becomes

$$\operatorname{Im}\Sigma_{\sigma}^{6(b)}(\omega,\mathbf{k}) \approx i^{6}\pi D^{2} \left\{ \int d\epsilon dE' d\phi d\phi' \frac{1}{q'^{2}} \delta\left(1 - \frac{|-\mathbf{k} + 2\mathbf{q}|}{q'}\right) \delta(\phi' - \phi_{-\mathbf{k} + 2\mathbf{q}}) \right.$$

$$\times \left[\delta(\omega + E' - 2\epsilon) - \delta(\omega + E' - 2\epsilon + u_{\mathbf{q}}) \right] \theta(\epsilon) \theta(-E')$$

$$- \int dE dE' d\phi d\phi' \frac{1}{q'^{2}} \delta\left(1 - \frac{|-\mathbf{k} + 2\mathbf{q}|}{q'}\right) \delta(\phi' - \phi_{-\mathbf{k} + 2\mathbf{q}})$$

$$\times \left[\delta(\omega + E' - 2E) - \delta(\omega + E' - 2E + u_{\mathbf{q}}) \right] \theta(-E) \theta(E') \right\}, \tag{34}$$

where we have four integrals and three delta functions, and we let $\delta(q'-|-\mathbf{k}+2\mathbf{q}|) \to \frac{1}{q'}\delta(1-\frac{|-\mathbf{k}+2\mathbf{q}|}{q'})$. We then consider the angle integral on ϕ' . In order to express $|-\mathbf{k}+2\mathbf{q}|, q, q'$ in terms of the integral variables and their corresponding angle dependence, we solve the equation $E(k,\phi_{\mathbf{k}})=E$ so that $k=f(E,\phi)$. Rewriting $u_{\mathbf{q}}=u_{q\phi}$, the approximate equation (34) becomes

$$\operatorname{Im}\Sigma_{\sigma}^{6(b)}(\omega,\mathbf{k}) \approx i^{6}\pi D^{2} \int d\phi' \delta(\phi' - \phi_{-\mathbf{k}+2\mathbf{q}})$$

$$\times \left\{ \int d\epsilon dE' d\phi \frac{1}{f^{2}(E',\phi')} \delta \left[1 - \frac{f(\epsilon,\phi_{-\mathbf{k}+2\mathbf{q}})}{f(E',\phi')} \right] \right.$$

$$\times \left[\delta(\omega + E' - 2\epsilon) - \delta(\omega + E' - 2\epsilon + u_{f(\epsilon,\phi),\phi}) \right] \theta(\epsilon) \theta(-E')$$

$$- \int dE dE' d\phi \frac{1}{f^{2}(E',\phi')} \delta \left[1 - \frac{f(E,\phi_{-\mathbf{k}+2\mathbf{q}})}{f(E',\phi')} \right]$$

$$\times \left[\delta(\omega + E' - 2E) - \delta(\omega + E' - 2E + u_{f(E,\phi),\phi}) \right] \theta(-E) \theta(E') \right\}. (35)$$

Performing the angle integral over ϕ' yields

$$\begin{split} \operatorname{Im} \Sigma_{\sigma}^{6(b)}(\omega,\mathbf{k}) &\approx i^{6} \pi D^{2} \Biggl\{ \int d\epsilon dE' d\phi \frac{1}{f^{2}(E',\phi_{-\mathbf{k}+2\mathbf{q}})} \delta \Biggl[1 - \frac{f(\epsilon,\phi_{-\mathbf{k}+2\mathbf{q}})}{f(E',\phi_{-\mathbf{k}+2\mathbf{q}})} \Biggr] \\ &\times \left[\delta(\omega+E'-2\epsilon) - \delta(\omega+E'-2\epsilon+u_{f(\epsilon,\phi),\phi}) \right] \theta(\epsilon) \theta(-E') \\ &- \int dE dE' d\phi \frac{1}{f^{2}(E',\phi_{-\mathbf{k}+2\mathbf{q}})} \delta \Biggl[1 - \frac{f(E,\phi_{-\mathbf{k}+2\mathbf{q}})}{f(E',\phi_{-\mathbf{k}+2\mathbf{q}})} \Biggr] \\ &\times \left[\delta(\omega+E'-2E) - \delta(\omega+E'-2E+u_{f(E,\phi),\phi}) \right] \theta(-E) \theta(E') \Biggr\}. \end{split}$$
(36)

We note that $\phi_{-\mathbf{k}+2\mathbf{q}}$ can be further replaced by another function g in terms of \mathbf{k} , ϵ , E and ϕ . Equation (35) becomes

$$\operatorname{Im}\Sigma_{\sigma}^{6(b)}(\omega,\mathbf{k}) \approx i^{6}\pi D^{2} \left\{ \int d\epsilon dE' d\phi \frac{1}{f^{2}[E',g(\mathbf{k},\epsilon,\phi)]} \delta \left\{ 1 - \frac{f[\epsilon,g(\mathbf{k},\epsilon,\phi)]}{f[E',g(\mathbf{k},\epsilon,\phi)]} \right\} \right.$$

$$\times \left[\delta(\omega+E'-2\epsilon) - \delta(\omega+E'-2\epsilon+u_{f(\epsilon,\phi),\phi}) \right] \theta(\epsilon) \theta(-E')$$

$$- \int dE dE' d\phi \frac{1}{f^{2}[E',g(\mathbf{k},E,\phi)]} \delta \left\{ 1 - \frac{f[E,g(\mathbf{k},E,\phi)]}{f[E',g(\mathbf{k},E,\phi)]} \right\}$$

$$\times \left[\delta(\omega+E'-2E) - \delta(\omega+E'-2E+u_{f(E,\phi),\phi}) \right] \theta(-E) \theta(E') \right\}. \tag{37}$$

We first perform the integral over ϕ . The remaining delta functions give us ϕ 's dependence on \mathbf{k} , ϵ , E and E', and we denote it as a function h. Hence, (37) becomes

Im
$$\Sigma_{\sigma}^{6(b)}(\omega, \mathbf{k})$$

$$\approx i^{6}\pi D^{2} \left\{ \int d\epsilon dE' \frac{1}{f^{2} \{E', g[\mathbf{k}, \epsilon, h(\mathbf{k}, \epsilon, E')]\}} \right.$$

$$\times \left[\delta(\omega + E' - 2\epsilon) - \delta(\omega + E' - 2\epsilon + u_{f[\epsilon, h(\mathbf{k}, \epsilon, E')], h(\mathbf{k}, \epsilon, E')}) \right] \theta(\epsilon) \theta(-E')$$

$$- \int dE dE' \frac{1}{f^{2} \{E', g[\mathbf{k}, E, h(\mathbf{k}, E, E')]\}}$$

$$\times \left[\delta(\omega + E' - 2E) - \delta(\omega + E' - 2E + u_{f[E, h(\mathbf{k}, E, E')], h(\mathbf{k}, E, E')}) \right] \theta(-E) \theta(E') \right\}. (38)$$

While we do not know the exact form of the terms $1/f^2$, they give us quantities of order $1/(\text{Fermi momentum})^2$, which is of order O(1) for generic lattice filling. Its dependence on ϵ , E, E' and \mathbf{k} is unimportant due to the phase space constraints, as will become clear soon. We are then left with integrals with energy variables ϵ , E and E':

$$\operatorname{Im}\Sigma_{\sigma}^{6(b)}(\omega,\mathbf{k}) \approx i^{6}\pi V^{2}D^{2} \times \left\{ \int d\epsilon dE'[\delta(\omega+E'-2\epsilon)-\delta(\omega+E'-2\epsilon) - \delta(\omega+E'-2\epsilon) - u_{f[\epsilon,h(\mathbf{k},\epsilon,E')],h(\mathbf{k},\epsilon,E')]}(\theta(\epsilon)\theta(-E') - \int dE dE'[\delta(\omega+E'-2E)-\delta(\omega+E'-2E) + u_{f[E,h(\mathbf{k},E,E')],h(\mathbf{k},E,E')]}(\theta(\epsilon)\theta(-E') \right\}.$$
(39)

We can then carry out the integral by assuming $u_{f[\epsilon,h(\mathbf{k},\epsilon,E')],h(\mathbf{k},\epsilon,E')}$ $\approx u_{f[E,h(\mathbf{k},E,E')],h(\mathbf{k},E,E')} \approx |u|$, where |u| is some constant average over $u_{f[\epsilon,h(\mathbf{k},\epsilon,E')],h(\mathbf{k},\epsilon,E')}$ or $u_{f[E,h(\mathbf{k},E,E')],h(\mathbf{k},E,E')}$. The integrals over E' give

$$\operatorname{Im}\Sigma_{\sigma}^{6(b)}(\omega, \mathbf{k}) \approx i^{6}\pi V^{2}D^{2} \left\{ \int d\epsilon \theta(\epsilon) [\theta(-2\epsilon + \omega) - \theta(-2\epsilon + \omega - |u|)] - \right.$$

$$\times \int dE \theta(E) [\theta(-2E + \omega) - \theta(-2E + \omega - |u|)] \right\}. \tag{40}$$

The integrals on ϵ , E give

$$\operatorname{Im}\Sigma_{\sigma}^{6(b)}(\omega, \mathbf{k}) \approx i^{6}\pi V^{2} \left[\left(\frac{\omega}{2} - \frac{\omega - |u|}{2} \right) - \left(\frac{\omega}{2} - \frac{\omega + |u|}{2} \right) \right]$$
(41)

$$= i^{6}\pi V^{2}D^{2} \left[\frac{|u|}{2} - \left(-\frac{|u|}{2} \right) \right] \tag{42}$$

$$= i^6 \pi V^2 D^2 |u|. (43)$$

Here, we note that the linearity in |u| comes from the energy integral per the phase space restrictions given by the step functions $\theta(-2\epsilon + \omega)$, $\theta(-2\epsilon + \omega - u_{\mathbf{q}})$, $\theta(E)$, and $\theta(-2E + \omega + u_{\mathbf{q}})$. The final result would not be exactly linear in |u|. Hence, we append a function $f(\mathbf{k})$ varying in \mathbf{k} :

$$\operatorname{Im}\Sigma_{\sigma}^{6(b)}(\omega, \mathbf{k}) \approx -\pi V^2 D^2 |u| f(\mathbf{k}), \tag{44}$$

where $f(\mathbf{k})$ is a dimensionless quantity of order O(1). Letting $\omega \to E_{\mathbf{k}\sigma}$, we obtain the self-energy results from other diagrams:

$$\operatorname{Im}\Sigma_{\sigma}^{6(f)}(\mathbf{k}) \approx -\frac{\pi}{2} V^2 D^2 u_{\mathbf{k}} (n_{\mathbf{k}\sigma} - n_{\mathbf{k}, -\sigma}), \tag{45}$$

$$\operatorname{Im}\Sigma_{\sigma}^{6(g)}(\mathbf{k}) \approx \operatorname{Im}\Sigma_{\sigma}^{6(h)}(\mathbf{k}) \approx \operatorname{Im}\Sigma_{\sigma}^{6(i)}(\mathbf{k}) \approx -\pi V^{2} D^{2} u_{\mathbf{k}} (n_{\mathbf{k}\sigma} - n_{\mathbf{k}, -\sigma})^{2}.$$
(46)

The rest imaginary parts resulting from Figs. 6(c), 6(d) and 6(e) share the same form but appear more complicated as we presented later in the appendix in the arXiv version. ¹² However, since we are only interested in the cases that occur near Fermi arcs and pseudo-Fermi surfaces, further simplifications can be done so that overall these imaginary parts results in zero or a quantity linear in u_k .

5. Summary and Discussions

In this paper, we studied the model introduced in Ref. 4 (referred to as HKY model) which gives rise to Fermi arcs and pseudogap, perturbed by Hubbard interaction. We found the combination of Hubbard and HKY interactions gives rise to a nonzero imaginary part to the electron self-energy in the low-energy limit. The origin of such non-Fermi liquid behavior lies in the singular nature of HKY interaction, which has infinite range in real space.

While our work was motivated by the cuprates, and gives rise to results that are qualitatively consistent with its phenomenology, the specific (and certainly

over-simplified) model we studied should not be taken as a realistic description of the physics of cuprates. Its value lies, instead, in

- (1) Its simplicity which demonstrates not only the possibility of Fermi arcs and pseudogap, but also that they go hand-in-hand with each other and with the observed non-Fermi liquid behavior. In fact, recent years have witnessed increasing activities in research using models that are extensions of the HK model^{8–11} aimed at understanding cuprate phenomenology, including superconductivity itself.
- (2) A starting point to build more realistic models for cuprates and other strongly correlated electron systems.

Acknowledgments

This work was supported by the National Science Foundation Grant No. DMR-1932796, and performed at the National High Magnetic Field Laboratory, which is supported by National Science Foundation Cooperative Agreement No. DMR-1644779, and the State of Florida.

References

- 1. C. Proust and L. Taillefer, Annu. Rev. Condens. Matter Phys. 10 (2019) 409.
- T. Yoshida, M. Hashimoto, I. M. Vishik, Z.-X. Shen and A. Fujimori, J. Phys. Soc. Jpn. 81 (2012) 011006.
- S. M. Girvin and K. Yang, Modern Condensed Matter Physics (Cambridge University Press, Cambridge, 2019), ISBN:9781107137394.
- 4. K. Yang, Phys. Rev. B 103 (2021) 024529.
- 5. Y. Hatsugai and M. Kohmoto, J. Phys. Soc. Jpn. 61 (1992) 2056.
- 6. G. Baskaran, Mod. Phys. Lett. B 5 (1991) 643.
- A. L. Fetter and J. D. Walecka, Quantum Theory of Many-Particle Systems (Courier Corporation, 2012).
- 8. P. W. Phillips, L. Yeo and E. W. Huang, Nat. Phys. 16 (2020) 1175.
- 9. R. D. Nesselrodt and J. K. Freericks, Phys. Rev. B 104 (2021) 155104.
- Y. Li, V. Mishra, Y. Zhou and F.-C. Zhang, New J. Phys. 24 (2022) 103019.
- 11. Y. Zhong, Phys. Rev. B 106 (2022) 155119.
- 12. R. Wang and K. Yang, arXiv: https://arxiv.org/abs/2301.045562301.04556.